

# Importance of considering helium excited states in $\text{He}^+$ scattering by an aluminum surface

A. Iglesias-García,<sup>1</sup> Evelina A. García,<sup>1</sup> and E. C. Goldberg<sup>1,2</sup>

<sup>1</sup>*Instituto de Física del Litoral (CONICET-UNL) Güemes 3450 (S3000GLN) Santa Fe, Argentina*

<sup>2</sup>*Departamento Ingeniería de Materiales, Facultad de Ingeniería Química, U.N.L., (S3000GLN) Santa Fe, Argentina*

(Received 5 May 2014; revised manuscript received 10 October 2014; published 13 November 2014)

The  $\text{He}^+$ /Al system is a very interesting projectile-surface combination which was thought initially as an example of a pure Auger neutralization mechanism. Then, because of the measured reionization explained by the antibonding interaction of the projectile state with the core target states, the resonant charge exchange with the band states was considered as another important contribution to the neutralization. Nevertheless, by only considering the neutralization to the ground state of helium, the measured ion survival probability is still overestimated. On the other hand, measurements of electron emission from an Al surface bombarded by He positive ions suggested the possibility of occupied excited states of helium due to the ion-surface collision. In this work, we also include the excited states of He within the time-dependent scattering process in which both neutralization mechanisms, resonant and Auger, are simultaneously contemplated. Our starting point is a multiorbital Anderson Hamiltonian projected over the selected space of ground and excited atomic configurations. An extra term related to the Auger mechanism is added to this Hamiltonian. A difference with previous works is that this approach includes the electron spin and, therefore, the spin fluctuation statistics in the charge-exchange process is correctly taken into account. We find a notable improvement in the agreement with the experiments and also that the interference between both mechanisms is not dramatic.

DOI: [10.1103/PhysRevB.90.195416](https://doi.org/10.1103/PhysRevB.90.195416)

PACS number(s): 79.20.Rf, 34.35.+a, 34.70.+e, 73.23.Hk

## I. INTRODUCTION

The measured charge fractions of ions scattered by surfaces and the electron emission produced due to the collision contain a rich physics related to the atom-surface interaction and, therefore, they provide a good test of any theoretical proposal about it. A lot of experimental and theoretical works show clearly that a successful atom-surface interaction model has to include the details of the surface electronic structure, the variation of the ion energy levels due to short- and long-range interactions, the electronic repulsion in the localized atomic states, and the all possible charge-exchange mechanisms [1–25].

The resonant and Auger processes are the two neutralization mechanisms involved in the time-dependent collision between ions and surfaces. In the first case, an electron tunneling process occurs when the atomic state resonates with a band state, and in this form one electron is transferred either from the atom to an empty band state or from an occupied band state to the atom. In the case of the Auger process, due to the electron-electron interaction in the solid, an electron from the valence band decays to the ion state and the liberated energy is transferred to another electron of the solid which can be emitted to the vacuum if the transferred energy is at least equal to the work function of the surface.

It has been believed until recently that the slow ions are Auger neutralized far from the surface at distances around 3–4 Å. In the case of the neutralization of slow noble gas ions, Hagstrum [26] introduced the distance- ( $z$ -) dependent Auger transition rate  $\Gamma(z) = \Gamma_0 \exp(-z/d)$ , where  $\Gamma_0$  and  $d$  are parameters which describe the Auger interaction for the ion-surface system. On the other hand, it has been found that collision-induced neutralization and reionization processes can occur close to the surface due to either bonding or antibonding interaction of the  $\text{He}(1s)$  level with the target core levels [6,12,27,28]. Then, resonant and Auger mechanisms

operating at very different regions of distances to the surface can be treated as independent processes [16]. Otherwise, if it is expected interferences, both mechanisms must be included together in the time-dependent evolution of the charge-transfer process [17,18,29].

In this work, we focus our attention in the collision of positive helium ions with a surface of aluminum, a system which has been widely studied but that still presents many interesting interrogates [14,17,18,22,30–35]. This collisional system was initially considered the perfect one for thinking in neutralization by an Auger mechanism [26], due to the relative position of the He ionization potential (24.6 eV) compared with the aluminum work function (4.43 eV). Nevertheless, the measured ion survival probability could not be well described by only assuming the Auger mechanism. Afterwards, the measured energy threshold for the reionization of neutral atoms [6,36] suggested strongly the activation of the resonant charge-exchange mechanism close to the surface region [16–18,22]. By taking into account this evidence, the resonant charge exchange promoted by the antibonding interaction between the  $\text{He-}1s$  state and the inner states of the target atom was also included in the dynamical evolution of the scattering process [17,18]. An important result obtained from these calculations was that the two mechanisms, acting at different distance regions, practically do not interfere. In this form, the theoretical ion survival probability was improved but not enough to achieve a good agreement with the experiments. All these calculations assume that the helium ground state is the only one active channel in the charge exchange with the band states of the surface. Nevertheless, there are other works that have suggested that the excited states of helium could be involved in the charge exchange with a metal surface [37–39]. On the other hand, there are experimental evidences of electron emission in the  $\text{He}^+$ /Al collision [22] that can be explained by a non-negligible population of the He excited states. In this work, Bajales *et al.* discussed the possible role of the

excited states in the  $\text{He}^+$  neutralization by performing a rough estimation of the neutral fraction. One important conclusion of this work was justly the necessity of a more exhaustive calculation of the neutral fraction by including excited states and the two possible neutralization mechanisms, resonant and Auger. In addition, we have recently shown that the practically complete neutralization observed in the scattering of  $\text{He}^+$  by a HOPG (highly oriented pyrolytic graphite) surface can be explained by correlation effects introduced by the first excited states of helium [25]. All these evidences led us to study the importance of the helium excited configurations in the  $\text{He}^+$  scattering by an Al surface.

The atom-surface interacting system is described by a multiorbital Anderson Hamiltonian projected over the selected space of electronic configurations of the helium atom, as in Ref. [25]. A new term that accounts for the mechanism of Auger neutralization to the ground state is added to the Hamiltonian in the present case. The dynamic process is solved by using nonequilibrium Green's functions calculated by means of the equation-of-motion method closed up to a second order in the atom-surface coupling. Our theoretical approach, applied to time-dependent collision processes in Ref. [25] and in this work, is also applicable to the description of many other nonequilibrium processes in condensed matter physics which involve strong correlated electrons and the interaction between localized and extended states. For instance, this kind of approach has been proven to be highly successful for describing the inelastic excitations and the Kondo physics in stationary processes such as the conductance through magnetic atoms, measured by using scanning tunneling microscopy [40,41].

This work is organized as follows: In Sec. II, we present and discuss the model Hamiltonian used for describing the atom-surface interaction. In Sec. III, the electronic configurations defining the atomic part of the Anderson Hamiltonian, the calculation of the energy and coupling terms of the Hamiltonian, and the Green's function formalism used for calculating the physical magnitudes of interest are discussed. In Sec. IV, we discuss our results obtained by going from the simplest description of the atom-surface interaction (spinless model) to the improved one involving many correlated charge-transfer channels and including spin fluctuation statistics. The interferences between Auger and resonant mechanisms along the time-dependent collision process are also discussed in this section. The concluding remarks are presented in Sec. V.

## II. MODEL HAMILTONIAN

The atom-surface interacting system is well described by the typical Anderson model [42] when the charge exchange occurs via a resonant tunneling process and there is only one active orbital in the atom. An extra term has to be added to the Anderson Hamiltonian for taking into account the Auger mechanism produced by electron-electron interactions, and the atomic part has to be extended in order to include many states in the atom. Then, the Hamiltonian can be separated in three terms:

$$\hat{H} = \hat{H}_{\text{sup}} + \hat{H}_{\text{ion/atom}} + \hat{H}_{\text{int}}, \quad (1)$$

where  $\hat{H}_{\text{sup}}$  describes the isolated solid,  $\hat{H}_{\text{ion/atom}}$  corresponds to the atomic system including the one- and two-electron interactions between the different orbitals, and finally the interaction term  $\hat{H}_{\text{int}}$  including the two charge-exchange mechanisms: resonant tunneling (one-electron term) and Auger (two-electron term). The respective expressions within a second quantization language are

$$\hat{H}_{\text{sup}} = \sum_{\vec{k}, \sigma} \varepsilon_{\vec{k}} \hat{c}_{\vec{k}\sigma}^\dagger \hat{c}_{\vec{k}\sigma}, \quad (2)$$

$$\begin{aligned} \hat{H}_{\text{ion/atom}} = & \sum_{m, \sigma} \zeta_m \hat{n}_{m\sigma} + \sum_m U_m \hat{n}_{m\uparrow} \hat{n}_{m\downarrow} \\ & + \frac{1}{2} \sum_{m \neq m', \sigma} J_{mm'} \hat{n}_{m\sigma} \hat{n}_{m'-\sigma} \\ & + \frac{1}{2} \sum_{m \neq m', \sigma} (J_{mm'} - J_{mm'}^x) \hat{n}_{m\sigma} \hat{n}_{m'\sigma} \\ & - \frac{1}{2} \sum_{m \neq m', \sigma} J_{mm'}^x \hat{c}_{m\sigma}^\dagger \hat{c}_{m'-\sigma} \hat{c}_{m'-\sigma}^\dagger \hat{c}_{m\sigma}, \quad (3) \end{aligned}$$

$$\begin{aligned} \hat{H}_{\text{int}} = & \sum_m \sum_{\vec{k}, \sigma} [V_{\vec{k}, m} \hat{c}_{\vec{k}, \sigma}^\dagger \hat{c}_{m, \sigma} + \text{H.c.}] \\ & + \sum_m \sum_{\substack{\vec{k} \neq \vec{k}' \neq \vec{k}'' \\ \sigma, \sigma'}} [V_{\vec{k}\vec{k}'\vec{k}'', m} \hat{c}_{\vec{k}\sigma}^\dagger \hat{c}_{\vec{k}'\sigma'}^\dagger \hat{c}_{\vec{k}''\sigma'} \hat{c}_{m\sigma} + \text{H.c.}]. \quad (4) \end{aligned}$$

In Eq. (2),  $\hat{c}_{\vec{k}\sigma}^\dagger$  creates an electron in a band state characterized by the wave vector  $\vec{k}$ , the spin projection  $\sigma$ , and the energy  $\varepsilon_{\vec{k}}$ . In Eq. (3),  $m$  denotes the atomic orbital,  $U$  and  $J$  are the direct Coulomb intra-atomic interactions, while  $J^x$  is the exchange one. The first term has to be with the kinetic energy and electron-nuclei potential, and the fifth term related with spin-flip processes restores the invariance under rotation in spin space. The first interaction term in Eq. (4) is the one corresponding to the resonant tunneling of an electron from the surface to the atom or vice versa due to the coupling between atomic and band states  $V_{\vec{k}, m}$ . The second term in Eq. (4) describes the Auger processes with matrix elements  $V_{\vec{k}\vec{k}'\vec{k}'', m} = \langle \vec{k}, \vec{k}' | \frac{1}{r-r'} | \vec{k}'' \phi_m \rangle$ , in which two electrons are destroyed (created) in the occupied (empty)  $m\sigma$  orbital of the atom and in the  $\vec{k}''$ -band state, respectively, and afterwards two electrons are created (destroyed) in empty (occupied) band states  $\vec{k}\sigma$  and  $\vec{k}'\sigma'$ . It should be kept in mind that states  $|\vec{k}\rangle$ ,  $|\vec{k}'\rangle$ , and  $|\vec{k}''\rangle$  have to be all different since we are describing a process in which a metal electron is transferred to the ion with simultaneous excitation of another metal electron. The total Hamiltonian [Eq. (1)] including many orbitals in the atom site [Eq. (3)] is solved by projecting it over the most probable electronic configurations of the atom, as it is discussed in the following section.

## III. INTERACTION OF CONFIGURATIONS: PROJECTION OPERATOR TECHNIQUE

The electronic configurations that can be probable neutralization channels of impinging ions  $\text{He}^+(1s)$  have been

discussed in the case of positive helium ions scattered by a HOPG surface [25]. These electronic configurations are eigenfunctions of the total spin projection  $S_z$ , which is a good quantum number in the scattering process of positive helium ions, and they are constructed from the one-electron orbitals ( $s$ ,  $p$ ) with well-defined spatial and spin variables. By using the Dirac notation, we have two spin degenerate ionic configurations  $|1s\sigma\rangle$  ( $S_z = \frac{1}{2}, -\frac{1}{2}$ ); one neutral configuration  $|1s\uparrow 1s\downarrow\rangle$  with  $S_z = 0$ ; two excited configurations  $|1s\sigma 2\alpha\sigma\rangle$  with  $S_z = 1$  and two  $|1s\bar{\sigma} 2\alpha\bar{\sigma}\rangle$  with  $S_z = -1$ , depending on the second electron is either in  $\alpha = 2s$  or  $2p$  orbital. Finally, four excited configurations  $|1s\sigma 2\alpha\bar{\sigma}\rangle$  with  $S_z = 0$ , two degenerate configurations corresponding to  $(1s2s)$ , and the other two corresponding to  $(1s2p)$ . The total energies of these electronic configurations are calculated accordingly to Eq. (3). Then, the  $S_z = 0$  configurations have a larger energy  $E(1s\sigma 2\alpha\bar{\sigma}) = \zeta_{1s} + \zeta_{2\alpha} + J_{1s2\alpha}$  than the ones with  $S_z = 1$  or  $-1$ , in which case the total energy is given by  $E(1s\sigma 2\alpha\sigma) = \zeta_{1s} + \zeta_{2\alpha} + J_{1s2\alpha} - J_{1s2\alpha}^x$ . We are including neither the  $\text{He}^{++}$  nor the  $\text{He}^-(1s2s2p)$  configurations because they are assumed less probable accordingly to an energetic criterion. By projecting the atomic part of the Hamiltonian [Eq. (3)] over the electronic configurations, we obtain

$$\begin{aligned} \hat{H}_{\text{ion/atom}} = & E(1s\uparrow) \sum_{\sigma} |1s\sigma\rangle \langle 1s\sigma| \\ & + E(1s^2) |1s\uparrow 1s\downarrow\rangle \langle 1s\uparrow 1s\downarrow| \\ & + \sum_{\sigma, \alpha=s,p} E(1s\sigma 2\alpha\sigma) |1s\sigma 2\alpha\sigma\rangle \langle 1s\sigma 2\alpha\sigma| \\ & + \sum_{\sigma, \alpha=s,p} E(1s\sigma 2\alpha\bar{\sigma}) |1s\sigma 2\alpha\bar{\sigma}\rangle \langle 1s\sigma 2\alpha\bar{\sigma}|, \end{aligned} \quad (5)$$

where  $E(\dots)$  are the total energies, and the interaction term of the Hamiltonian [Eq. (4)] results to be

$$\begin{aligned} \hat{H}_{\text{int}} = & \sum_{\bar{k}} [\tilde{V}_{\bar{k}1s} \hat{c}_{\bar{k}\uparrow}^\dagger |1s\downarrow\rangle \langle 1s\uparrow 1s\downarrow| + \text{H.c.}] \\ & - \sum_{\bar{k}} [\tilde{V}_{\bar{k}1s} \hat{c}_{\bar{k}\downarrow}^\dagger |1s\uparrow\rangle \langle 1s\uparrow 1s\downarrow| + \text{H.c.}] \\ & - \sum_{\bar{k}, \sigma, \alpha=s,p} [V_{\bar{k}2\alpha} \hat{c}_{\bar{k}\sigma}^\dagger |1s\sigma\rangle \langle 1s\sigma 2\alpha\sigma| + \text{H.c.}] \\ & - \sum_{\bar{k}, \sigma, \alpha=s,p} [V_{\bar{k}2\alpha} \hat{c}_{\bar{k}\bar{\sigma}}^\dagger |1s\sigma\rangle \langle 1s\sigma 2\alpha\bar{\sigma}| + \text{H.c.}] \\ & + \sum_{\bar{k} \neq \bar{k}' \neq \bar{k}'' \sigma} [\tilde{V}_{\bar{k}\bar{k}'\bar{k}''\sigma} \hat{c}_{\bar{k}\uparrow}^\dagger \hat{c}_{\bar{k}'\sigma}^\dagger \hat{c}_{\bar{k}''\sigma} |1s\downarrow\rangle \langle 1s\uparrow 1s\downarrow| + \text{H.c.}] \\ & - \sum_{\bar{k} \neq \bar{k}' \neq \bar{k}'' \sigma} [\tilde{V}_{\bar{k}\bar{k}'\bar{k}''\sigma} \hat{c}_{\bar{k}\downarrow}^\dagger \hat{c}_{\bar{k}'\sigma}^\dagger \hat{c}_{\bar{k}''\sigma} |1s\uparrow\rangle \langle 1s\uparrow 1s\downarrow| + \text{H.c.}] \end{aligned} \quad (6)$$

In Eq. (6), the first two terms and the last two related to the Auger process take into account the spin fluctuation statistics in the charge exchange between the helium ground state and the surface states. This is an improvement with respect to previous

works [17,18], in which the electron spin was disregarded. The hopping renormalization  $\tilde{V}_{\bar{k}1s} = V_{\bar{k}1s}/\sqrt{N}$  and  $\tilde{V}_{\bar{k}\bar{k}'\bar{k}''\sigma} = V_{\bar{k}\bar{k}'\bar{k}''\sigma}/\sqrt{N}$  is related to the spin degeneration ( $N = 2$ ). The neutralization to the excited configurations is predominantly occurring by a resonant charge exchange between atom and band states [third and fourth terms in Eq. (6)] due to the relative energy levels positions, and because it takes place in a shorter time than the Auger mechanism.

### A. Energy and hopping parameters

The one-electron energy levels are defined as the difference between the total energies of the system with  $N + 1$  and  $N$  electrons. In this form, we can define the one-electron energy for the neutralization of  $\text{He}^+(1s)$  to the ground state as  $\varepsilon_{1s} = E(1s\uparrow 1s\downarrow) - E(1s\uparrow) = E(1s\uparrow 1s\downarrow) - E(1s\downarrow)$ .

On the other hand,  $\text{He}^+(1s\sigma)$  can be neutralized to the excited state  $1s2\alpha\sigma$  with a  $z$  component of the total spin  $S_z = 1, -1$  or to the excited state  $1s2\alpha\bar{\sigma}$  with  $S_z = 0$ , each one representing two energy degenerate possibilities. The one-electron energies associated with these charge-spin fluctuations are given by  $\varepsilon_{2\alpha\sigma} = E(1s\sigma 2\alpha\sigma) - E(1s\sigma)$  and  $\varepsilon_{2\alpha\bar{\sigma}} = E(1s\sigma 2\alpha\bar{\sigma}) - E(1s\sigma)$ .

The atom energy and the hopping terms are obtained from a model developed for describing the adiabatic interaction between an atom and a surface, based on both localized and extended features of the interacting system [43]. Basically, a linear combination of atomic orbitals (LCAO) of the surface band states and a mean-field approximation of the two-electron interaction terms are performed. The effect of the long-range interactions is introduced by considering the image potential defining the energy-level shift for large normal distances ( $z$ ) to the surface ( $z > 8$  a.u.). The image plane position in the case of Al(100) surface is  $z_I = 3.5$  a.u. We used the atomic basis for Al and He atoms provided in Ref. [44]. The  $2s$  and  $2p$  Gaussian orbitals used for He atom [45] approximate well the energy of the first excited state  $^3S$  of He, 19.73 eV against the experimental value equal to 19.82 eV, and also to the energy of the excited state  $^3P$ , 20.5 eV compared with the experimental value 20.96 eV [46].

In Fig. 1, we show the variation with the distance to the surface of the one-electron energy levels associated to the different neutralization channels and referred to the Fermi energy of Al(100); the surface local density of states is also included in the figure [47,48]. It is considered the interaction of He atom with the scatter aluminum atom and its first neighbors (see inset in Fig. 1), which were found to be active in the case of the interaction of the excited states with the surface. The more localized nature of the He- $1s$  state makes its energy level practically insensitive to the interaction with many substrate atoms. The energy levels have been rigidly shifted a little in order to have asymptotic values equal to the corresponding ones for the isolated He atom [46].

After the upward shift caused by the image potential at large distances, the short-range interactions with many Al atoms diminish the energy of the levels associated with the neutralization to excited states, locating them below the Fermi level. This fact makes possible the formation of excited neutral atoms at distances close to the surface whose survival probability will depend mainly on the projectile velocity.

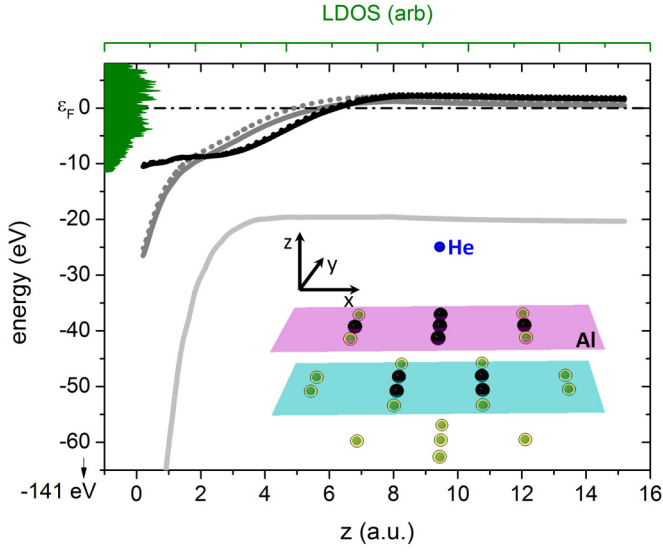


FIG. 1. (Color online) One-electron energy levels as a function of ion-surface distance.  $\epsilon_{1s}$  (light gray line);  $\epsilon_{2s}$  (solid dark gray line);  $\epsilon_{2s\sigma}$  (dotted dark gray line);  $\epsilon_{2p_z}$  (solid black line);  $\epsilon_{2p_z\sigma}$  (dotted black line). Fermi energy  $\epsilon_F = 0$  is indicated by a dashed-dotted line. The shadowed region corresponds to the local density of states (LDOS) of Al(100). Inset: the ion projectile in front of the surface and the active nine substrate atoms considered (black spheres).

The LCAO expansion of the  $\psi_{\vec{k}}$  states in the atomic orbitals  $\phi_i(\vec{r} - \vec{R}_s)$  allows writing [43]

$$\begin{aligned} \hat{V}_{\vec{k}\beta}(\vec{R}) &= \sum_{i, \vec{R}_s} c_{i, \vec{R}_s}^{\vec{k}} \langle \phi_i(\vec{r} - \vec{R}_s) | \hat{V} | \varphi_{\beta}(\vec{r} - \vec{R}) \rangle \\ &= \sum_{i, \vec{R}_s} c_{i, \vec{R}_s}^{\vec{k}} V_{i, \vec{R}_s; \beta}, \end{aligned}$$

which is a superposition of the atom-atom couplings weighted by the coefficients  $c_{i, \vec{R}_s}^{\vec{k}}$  that define the density matrix of the solid  $[\vec{R}$  is the projectile atom position with respect to the scatter surface atom which defines the origin of coordinates  $\vec{R}_s = (0, 0, 0)$ ]:

$$\rho_{i, \vec{R}_s; j, \vec{R}_s'}(\epsilon) = \sum_{\vec{k}} c_{i, \vec{R}_s}^{\vec{k}*} c_{j, \vec{R}_s'}^{\vec{k}} \delta(\epsilon - \epsilon_{\vec{k}}).$$

In this form, the localized nature of the atoms and the extended features of the surface enter in the calculation of the charge exchange between ions and surfaces. The core bands of the surface are also included by considering them as zero-width bands. It is found a significant coupling of the He-1s orbital with the core states of Al that makes possible the promotion of the helium ionization level and allows for a little chance of a resonant neutralization. Accordingly to the extended behavior of the coupling with the valence states of Al, we consider the first eight neighbors of the Al scatter atom in the LCAO expansion of the  $\psi_{\vec{k}}$  states (see inset of Fig. 1).

## B. Calculation of the atom charge state probabilities

The probability of ion survival is given by

$$n_{\text{He}^+} = \sum_{\sigma} \langle |1s\sigma\rangle \langle 1s\sigma| \rangle,$$

while the probabilities of having the atom in neutral configurations are

$$n_{\text{He}^0(1s^2)} = \langle |1s\uparrow 1s\downarrow\rangle \langle 1s\uparrow 1s\downarrow| \rangle$$

in the case of the ground state, and

$$n_{\text{He}^0(1s2\alpha,1)} = \sum_{\sigma} \langle |1s\sigma 2\alpha\sigma\rangle \langle 1s\sigma 2\alpha\sigma| \rangle,$$

$$n_{\text{He}^0(1s2\alpha,0)} = \sum_{\sigma} \langle |1s\sigma 2\alpha\bar{\sigma}\rangle \langle 1s\sigma 2\alpha\bar{\sigma}| \rangle$$

in the case of excited states with  $S_z = 1, -1$  or  $S_z = 0$ , respectively.

The time evolution of the average occupation of each atomic configuration is calculated by using the equation of motion in the Heisenberg picture (atomic units are used), as  $d\langle \hat{n} \rangle / dt = -i\langle [\hat{n}, \hat{H}] \rangle$ . By taking into account the energy degeneration and the normalization of the selected subspace

$$n_{\text{He}^+} + n_{\text{He}^0(1s^2)} + \sum_{\alpha=s,p} [n_{\text{He}^0(1s2\alpha,1)} + n_{\text{He}^0(1s2\alpha,0)}] = 1,$$

it is enough to calculate

$$\begin{aligned} & \frac{d\langle |1s\uparrow 1s\downarrow\rangle \langle 1s\uparrow 1s\downarrow| \rangle}{dt} \\ &= 4 \text{Im} \left[ \sum_{\vec{k}} \tilde{V}_{\vec{k}1s}^* \langle |1s\uparrow 1s\downarrow\rangle \langle 1s\downarrow | \hat{c}_{\vec{k}\uparrow}^\dagger \rangle \right. \\ & \quad \left. + \sum_{\vec{k} \neq \vec{k}' \neq \vec{k}''\sigma} \tilde{V}_{\uparrow \vec{k} \vec{k}' \vec{k}''} \langle |1s\uparrow 1s\downarrow\rangle \langle 1s\downarrow | c_{\vec{k}'\sigma}^\dagger c_{\vec{k}\sigma} c_{\vec{k}\downarrow} \rangle \right], \quad (7) \end{aligned}$$

$$\begin{aligned} & \frac{d\langle |1s\uparrow 2\alpha\uparrow\rangle \langle 1s\uparrow 2\alpha\uparrow| \rangle}{dt} \\ &= -2 \text{Im} \sum_{\vec{k}} V_{\vec{k}2\alpha}^* \langle |1s\uparrow 2\alpha\uparrow\rangle \langle \uparrow 0 | \hat{c}_{\vec{k}\uparrow}^\dagger \rangle, \quad (8) \end{aligned}$$

$$\begin{aligned} & \frac{d\langle |1s\uparrow 2\alpha\downarrow\rangle \langle 1s\uparrow 2\alpha\downarrow| \rangle}{dt} \\ &= -2 \text{Im} \sum_{\vec{k}} V_{\vec{k}2\alpha}^* \langle |1s\uparrow 2\alpha\uparrow\rangle \langle \uparrow 0 | \hat{c}_{\vec{k}\uparrow}^\dagger \rangle. \quad (9) \end{aligned}$$

The first term in Eq. (7) takes into account the contribution of the resonant charge transfer to the ground state while the second term is accounting for the Auger neutralization process. The occupation of the excited configurations is determined only by the resonant charge-exchange mechanism [Eqs. (8) and (9)].

The calculation of the crossed terms in the case of the resonant processes  $\langle |A\rangle \langle B | \hat{c}_{\vec{k}\sigma}^\dagger \rangle$  has been largely discussed in Ref. [25]. These ones are calculated by using that

$$\langle |A\rangle \langle B | c_{\vec{k}\sigma}^\dagger \rangle = (1/2) i F_{|A\rangle \langle B |} (\hat{c}_{\vec{k}\sigma}^\dagger)_{t=t'},$$

where  $F_{|A\rangle\langle B|}(\hat{c}_{\vec{k}\sigma})$  is given by

$$F_{|A\rangle\langle B|}(\hat{c}_{\vec{k}\sigma})_{t=t'} = -i \int_{t_0}^t d\tau V_{\vec{k}\beta} [F_{|A\rangle\langle B|}(\tau, t) - (2\langle \hat{n}_{\vec{k}\sigma} \rangle - 1)G_{|A\rangle\langle B|}(\tau, t)] e^{i\varepsilon_{\vec{k}}(\tau-t)}. \quad (10)$$

$\langle \hat{n}_{\vec{k}\sigma} \rangle$  corresponds to the Fermi function at a temperature  $T$ . The Green's functions that appear in Eq. (10) are the typical ones of the Keldysh formalism [49] but written in the projection operator language:

$$G_{|A\rangle\langle B|}(\tau, t) = i\Theta(t - \tau)\langle [|A\rangle\langle B|(t); |B\rangle\langle A|(\tau)] \rangle, \quad (11)$$

$$F_{|A\rangle\langle B|}(\tau, t) = i\langle [|A\rangle\langle B|(t); |B\rangle\langle A|(\tau)] \rangle,$$

where  $[\dots; \dots]$  and  $\{\dots; \dots\}$  indicate commutator and anti-commutator, respectively.

The crossed terms related to the Auger process can be calculated by following a similar procedure:

$$\langle |A\rangle\langle B| c_{\vec{k}'\sigma}^\dagger c_{\vec{k}'\sigma} c_{\vec{k}\sigma} \rangle = (1/2)i F_{|A\rangle\langle B|}(\hat{c}_{\vec{k}'\sigma}^\dagger \hat{c}_{\vec{k}'\sigma} \hat{c}_{\vec{k}\sigma})_{t=t'},$$

being  $A = 1s\uparrow 1s\downarrow$  y  $B = 1s\downarrow$  and

$$F_{|A\rangle\langle B|}(\hat{c}_{\vec{k}'\sigma}^\dagger \hat{c}_{\vec{k}'\sigma} \hat{c}_{\vec{k}\sigma}) = i\langle [|A\rangle\langle B|; \hat{c}_{\vec{k}'\sigma}^\dagger \hat{c}_{\vec{k}'\sigma} \hat{c}_{\vec{k}\sigma}] \rangle.$$

The equation of motion of the Green's function  $F_{|A\rangle\langle B|}(\hat{c}_{\vec{k}'\sigma}^\dagger \hat{c}_{\vec{k}'\sigma} \hat{c}_{\vec{k}\sigma})$  leads to the following expression in terms of the Green's functions [Eq. (11)]:

$$\begin{aligned} F_{|A\rangle\langle B|}(\hat{c}_{\vec{k}'\sigma}^\dagger \hat{c}_{\vec{k}'\sigma} \hat{c}_{\vec{k}\sigma})_{t=t'} &= i[\langle n_{\vec{k}\uparrow} \rangle \langle n_{\vec{k}'\sigma} \rangle \langle 1 - n_{\vec{k}'\sigma} \rangle + \langle n_{\vec{k}'\sigma} \rangle \langle 1 - n_{\vec{k}'\sigma} \rangle \langle 1 - n_{\vec{k}\uparrow} \rangle] \\ &\times \int_{t_0}^t d\tau \tilde{V}_{\vec{k}'\vec{k}\vec{k}\uparrow}(\tau) [(2n_{\vec{k}\uparrow} - 1)G_{|A\rangle\langle B|}(\tau, t) \\ &- F_{|A\rangle\langle B|}(\tau, t)] e^{i(\varepsilon_{\vec{k}'\sigma} - \varepsilon_{\vec{k}\uparrow} - \varepsilon_{\vec{k}'\sigma})(\tau-t)}. \end{aligned} \quad (12)$$

Finally, we have to calculate the Green's functions  $G_{|A\rangle\langle B|}(\tau, t)$  and  $F_{|A\rangle\langle B|}(\tau, t)$ . We employed the equation-of-motion method together with a closure criterion based on a second order in the coupling term and a mean-field approximation [25]. We can separate the Auger and resonant contributions to the time derivative of the Green's functions:

$$\frac{dG(F)}{dt} = \frac{dG(F)}{dt} \Big|_{\text{resonant}} + \frac{dG(F)}{dt} \Big|_{\text{Auger}}.$$

The contribution of the resonant terms is detailed in Ref. [25]. In the case of neutralization to the ground state  $A = 1s\uparrow 1s\downarrow$  and  $B = 1s\uparrow$ , we have

$$\begin{aligned} i \frac{dg_{|A\rangle\langle B|}(t, t')}{dt} \Big|_{\text{Auger}} &= \sum_{\vec{k} \neq \vec{k}' \neq \vec{k}''\sigma} \tilde{V}_{\uparrow\vec{k}'\vec{k}\vec{k}}(t) \langle |1s\uparrow 1s\downarrow\rangle \langle 1s\downarrow | c_{\vec{k}'\sigma}^\dagger c_{\vec{k}'\sigma} c_{\vec{k}\uparrow} | \rangle_{t'} e^{-i(\varepsilon_{\vec{k}\uparrow} + \varepsilon_{\vec{k}'\sigma} - \varepsilon_{\vec{k}'\sigma})(t-t')} e^{i \int_{t'}^t \varepsilon_{1s} dx} \\ &+ i \int_{-\infty}^{\infty} d\tau [\Xi_C(t, \tau) + 2\Xi_L(t, \tau)] e^{-i \int_{t'}^{\tau} \varepsilon_{1s} dx} g_{|A\rangle\langle B|}(\tau, t'), \end{aligned} \quad (13)$$

$$\begin{aligned} i \frac{df_{|A\rangle\langle B|}(t, t')}{dt} \Big|_{\text{Auger}} &= \sum_{\vec{k} \neq \vec{k}' \neq \vec{k}''\sigma} (2n_{\vec{k}\uparrow} - 1) \tilde{V}_{\uparrow\vec{k}'\vec{k}\vec{k}}(t) \langle |1s\uparrow 1s\downarrow\rangle \langle 1s\downarrow | c_{\vec{k}'\sigma}^\dagger c_{\vec{k}'\sigma} c_{\vec{k}\uparrow} | \rangle_{t'} e^{-i(\varepsilon_{\vec{k}\uparrow} + \varepsilon_{\vec{k}'\sigma} - \varepsilon_{\vec{k}'\sigma})(t-t')} e^{i \int_{t'}^t \varepsilon_{1s} dx} \\ &+ i \int_{-\infty}^{\infty} d\tau [\Xi_C(t, \tau) + 2\Xi_L(t, \tau)] e^{-i \int_{t'}^{\tau} \varepsilon_{1s} dx} f_{|A\rangle\langle B|}(\tau, t') \\ &+ i \int_{-\infty}^{\infty} d\tau [\Omega_C(t, \tau) + 2\Omega_L(t, \tau)] e^{-i \int_{t'}^{\tau} \varepsilon_{1s} dx} g_{|A\rangle\langle B|}(\tau, t'). \end{aligned} \quad (14)$$

The neutralization to the excited states is indirectly affected by the Auger mechanism of neutralization only assumed operative for the ground state. In this case,  $A = 1s\uparrow 2\alpha\sigma$  and  $B = 1s\uparrow$ , the contribution of the Auger terms to the total Green's function is given by

$$\begin{aligned} i \frac{dg_{|A\rangle\langle B|}(t, t')}{dt} \Big|_{\text{Auger}} &= \sum_{\vec{k} \neq \vec{k}' \neq \vec{k}''\sigma} \tilde{V}_{\uparrow\vec{k}'\vec{k}\vec{k}}(t) \langle |1s\uparrow 1s\downarrow\rangle \langle 1s\downarrow | c_{\vec{k}'\sigma}^\dagger c_{\vec{k}'\sigma} c_{\vec{k}\uparrow} | \rangle_{t'} e^{-i(\varepsilon_{\vec{k}\uparrow} + \varepsilon_{\vec{k}'\sigma} - \varepsilon_{\vec{k}'\sigma})(t-t')} e^{i \int_{t'}^t \varepsilon_{1s} dx} \\ &+ i \int_{-\infty}^{\infty} d\tau \Xi_C(t, \tau) e^{-i \int_{t'}^{\tau} \varepsilon_{1s} dx} g_{|A\rangle\langle B|}(\tau, t'), \end{aligned} \quad (15)$$

$$\begin{aligned} i \frac{df_{|A\rangle\langle B|}(t, t')}{dt} \Big|_{\text{Auger}} &= \sum_{\vec{k} \neq \vec{k}' \neq \vec{k}''\sigma} (2n_{\vec{k}\uparrow} - 1) \tilde{V}_{\uparrow\vec{k}'\vec{k}\vec{k}}(t) \langle |1s\uparrow 1s\downarrow\rangle \langle 1s\downarrow | c_{\vec{k}'\sigma}^\dagger c_{\vec{k}'\sigma} c_{\vec{k}\uparrow} | \rangle_{t'} e^{-i(\varepsilon_{\vec{k}\uparrow} + \varepsilon_{\vec{k}'\sigma} - \varepsilon_{\vec{k}'\sigma})(t-t')} e^{i \int_{t'}^t \varepsilon_{1s} dx} \\ &+ i \int_{-\infty}^{\infty} d\tau \Xi_C(t, \tau) e^{-i \int_{t'}^{\tau} \varepsilon_{1s} dx} f_{|A\rangle\langle B|}(\tau, t') + i \int_{-\infty}^{\infty} d\tau \Omega_C(t, \tau) e^{-i \int_{t'}^{\tau} \varepsilon_{1s} dx} g_{|A\rangle\langle B|}(\tau, t'). \end{aligned} \quad (16)$$

The phase transformation

$$G(F)_{|A\rangle\langle B|}(t,t') = e^{-i \int_{t'}^t [E(|A\rangle) - E(|B\rangle)] d\tau} g(f)_{|A\rangle\langle B|}(t,t')$$

has been performed in all the expressions before [Eqs. (13)–(16)]. Notice that the crossed term ( $\langle |1s\uparrow 1s\downarrow\rangle \langle 1s\downarrow | c_{\vec{k}'\sigma}^\dagger c_{\vec{k}\sigma} c_{\vec{k}\sigma} c_{\vec{k}'\sigma} | \rangle_{t'}$ ) is appearing in the motion equation of the Green's functions, which marks a difference with respect to Refs. [17,18]. This new term is associated to the spin fluctuation statistics we are considering in this work.

The Auger self-energies for capture [ $\Xi_C(t,\tau)$ ,  $\Omega_C(t,\tau)$ ] and loss [ $\Xi_L(t,\tau)$ ,  $\Omega_L(t,\tau)$ ] processes introduced in Eqs. (13)–(16) are given by (we neglect the exchange terms)

$$\begin{aligned} \Xi_C(t,\tau) &= i\Theta(\tau-t) \sum_{\vec{k}\neq\vec{k}'\neq\vec{k}''\sigma} \tilde{V}_{\vec{k}''\vec{k}'\vec{k}\downarrow}^*(t) \tilde{V}_{\vec{k}''\vec{k}'\vec{k}\downarrow}(\tau) \langle n_{\vec{k}\downarrow} \rangle \langle n_{\vec{k}'\sigma} \rangle \langle 1 - n_{\vec{k}''\sigma} \rangle e^{i(\varepsilon_{\vec{k}\downarrow} + \varepsilon_{\vec{k}'\sigma} - \varepsilon_{\vec{k}''\sigma})(\tau-t)}, \\ \Xi_L(t,\tau) &= i\Theta(\tau-t) \sum_{\vec{k}\neq\vec{k}'\neq\vec{k}''\sigma} \tilde{V}_{\vec{k}''\vec{k}'\vec{k}\uparrow}^*(t) \tilde{V}_{\vec{k}''\vec{k}'\vec{k}\uparrow}(\tau) \langle n_{\vec{k}\sigma} \rangle \langle 1 - n_{\vec{k}'\sigma} \rangle \langle 1 - n_{\vec{k}\uparrow} \rangle e^{i(\varepsilon_{\vec{k}\uparrow} + \varepsilon_{\vec{k}'\sigma} - \varepsilon_{\vec{k}''\sigma})(\tau-t)}, \\ \Omega_C(t,\tau) &= i \sum_{\vec{k}\neq\vec{k}'\neq\vec{k}''\sigma} \tilde{V}_{\vec{k}''\vec{k}'\vec{k}\downarrow}^*(t) \tilde{V}_{\vec{k}''\vec{k}'\vec{k}\downarrow}(\tau) (2n_{\vec{k}\downarrow} - 1) \langle n_{\vec{k}\downarrow} \rangle \langle n_{\vec{k}'\sigma} \rangle \langle 1 - n_{\vec{k}''\sigma} \rangle e^{i(\varepsilon_{\vec{k}\downarrow} + \varepsilon_{\vec{k}'\sigma} - \varepsilon_{\vec{k}''\sigma})(\tau-t)}, \\ \Omega_L(t,\tau) &= i \sum_{\vec{k}\neq\vec{k}'\neq\vec{k}''\sigma} \tilde{V}_{\vec{k}''\vec{k}'\vec{k}\uparrow}^*(t) \tilde{V}_{\vec{k}''\vec{k}'\vec{k}\uparrow}(\tau) (2n_{\vec{k}\uparrow} - 1) \langle n_{\vec{k}''\sigma} \rangle \langle 1 - n_{\vec{k}'\sigma} \rangle \langle 1 - n_{\vec{k}\uparrow} \rangle e^{i(\varepsilon_{\vec{k}\uparrow} + \varepsilon_{\vec{k}'\sigma} - \varepsilon_{\vec{k}''\sigma})(\tau-t)}. \end{aligned} \quad (17)$$

The factor 2 that appears multiplying the self-energies related to the loss processes in Eqs. (13) and (14) is due to the spin fluctuation statistics; the loss process ( $\text{He}^0 \rightarrow \text{He}^+$ ) has double the chances than the capture one ( $\text{He}^+ \rightarrow \text{He}^0$ ).

The final expressions of the Auger self-energies are obtained by following the procedure detailed in Refs. [17,18]. The surface is taken into account by using the second ansatz of Ref. [18]:

$$\Xi_{C,L}(t,t') = \Xi_{C,L}^{vol}(t-t') f(t) f(t'),$$

with  $f(t)$  given by

$$f(t) = \begin{cases} e^{-[z(t)-z_j]/2d} & \text{if } z > z_j, \\ 1 & \text{if } z < z_j, \end{cases} \quad (18)$$

where  $z_j = 2$  a.u. is the jellium edge position and  $d = 1.15$  a.u.

#### IV. RESULTS AND DISCUSSION

In the previous works [17,18], the scattering angles  $180^\circ$  and  $135^\circ$  were used indistinctly and it was found practically no differences between both backscattering situations. In this work, we choose a scattering angle of  $180^\circ$  with a normal incidence which is the more appropriate scattering geometry for our model calculation. In this case, by taking into account the energy loss factor calculated for a scattering angle of  $180^\circ$ , the ion energy in the outgoing path ( $E_{\text{out}}$ ) is 0.55 times the incoming energy ( $E_{\text{in}}$ ). The turning points of the ion trajectory are determined from the He-Al interaction energy and vary from 0.5 a.u. for the minimum incident energy value considered (450 eV) to 0.2 a.u. for the maximum value considered (3000 eV). The quantity measured is the ion fraction and it will be compared with our theoretical results  $P^+ = 1 - n_{\text{He}^0(1s^2)} - \sum_{\alpha=s,p} [n_{\text{He}^0(1s2\alpha,1)} + n_{\text{He}^0(1s2\alpha,0)}]$ .

#### A. The ground state as the unique neutralization channel

The neutralization probability is given by the occupation of the only one active state He-1s assumed in this approximation. In this case, the calculation of the ion survival probability is done in the first place by ignoring the electron spin (spinless approximation) as in previous works [17,18], and then by including the spin fluctuation statistics.

In Fig. 2, we compare the calculated ion fraction by using the spinless approximation, as a function of the ion inverse velocity, with the experimental results shown in previous works [16,17]. In this figure, from the analysis of the ion survival probability by considering either the Auger or the resonant mechanism alone, we observe that the

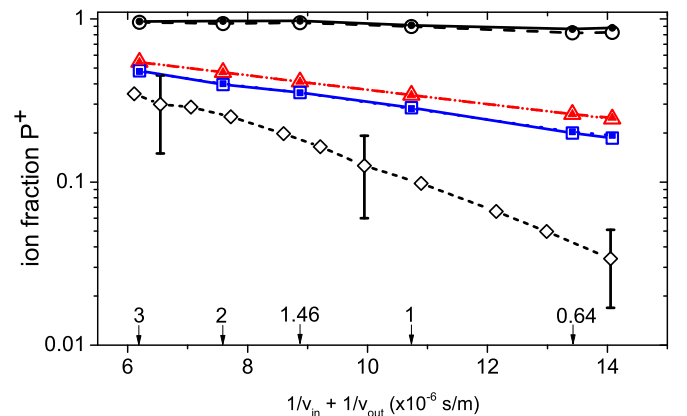


FIG. 2. (Color online) Spinless calculation of the ion fraction as a function of the inverse perpendicular velocity for the incoming (in) and outgoing (out) trajectories. Auger mechanism (triangles); resonant mechanism (circles); both mechanisms (squares). Full symbols: by including spin fluctuations. The diamonds correspond to the experimental data [17]. Incident kinetic energies (in keV) are indicated by arrows on the lower x axis.

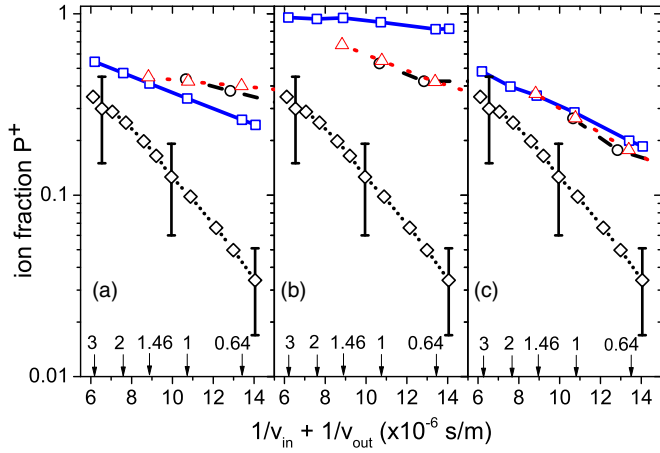


FIG. 3. (Color online) Spinless calculation of the ion fraction as a function of the inverse ion velocity. This work (squares), Ref. [17] (circles), Ref. [18] (triangles). (a) Auger, (b) resonant, (c) both Auger + resonant. The diamonds correspond to the experimental data [17]. Incident kinetic energies (in keV) are indicated by arrows on the lower  $x$  axis.

resonant mechanism contributes very little to the ground-state neutralization.

The calculated ion fraction by including the spin fluctuations is also shown in Fig. 2. In this calculation, the resonant charge-exchange process is described by the first two terms of Eq. (6) and it is equivalent to an infinite correlation limit approximation. Only slight differences by considering the spin fluctuations are observed. The tendency is to increase the ion survival probability due to the two possibilities of electron loss introduced by the spin statistics [see Eqs. (13) and (14)], but in this case the loss processes are very improbable due to the large ionization energy of helium.

In Fig. 3, we compare the results of this work with those of previous works [17,18] calculated by using the spinless approximation for different scattering angles:  $135^\circ$  in Ref. [17] and  $180^\circ$  in Ref. [18]. It can be seen that the total ion fractions are very similar [Fig. 3(c)]. Nevertheless, when we analyze separately each mechanism, we find that the present calculations lead to a larger Auger neutralization [Fig. 3(a)] and to a smaller resonant one [Fig. 3(b)]. We can understand this result from the difference between the parameters used in this work and those used in Refs. [17,18]. The major flexibility of the atomic basis ( $1s, 2s, 2p$ ) used in this work leads to a more pronounced falldown of the ionization level near the surface and to smaller coupling integrals. Then, a larger ionization energy favors the Auger neutralization while the resonant mechanism becomes less probable due to the smaller values of both the He( $1s$ ) energy and the coupling integrals.

### B. Calculation including the resonant charge exchange with helium excited states

The successive calculations of the ion fraction are shown in Fig. 4: by only considering the Auger process, by including the resonant neutralization to the ground state, and finally, by including also the resonant neutralization to the excited states of helium. We can see that the agreement with the experiment

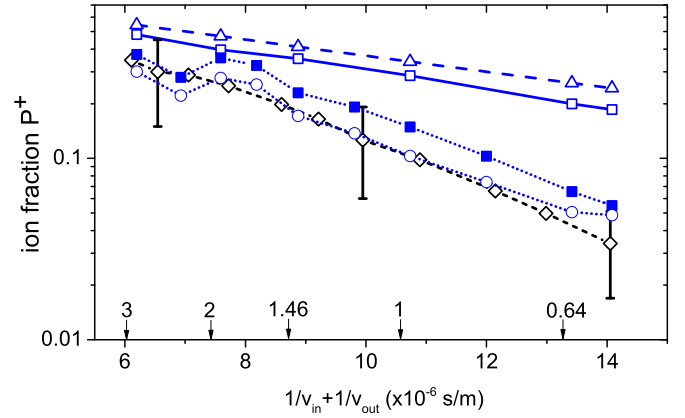


FIG. 4. (Color online) Ion fraction as a function of the inverse ion velocity, by including the different neutralization channels. Only Auger (triangles); resonant and Auger neutralization to the ground state (empty squares); by including also the resonant neutralization to the excited states (solid squares). The diamonds correspond to the experimental data [17]. Incident kinetic energies (in keV) are indicated by arrows on the lower  $x$  axis. The circle symbols correspond to the ion fraction calculated by using the semiclassical approximation (see the text).

is largely improved when the interaction between the atom excited states and the surface band states is taken into account.

In Fig. 4, we also show the ion fraction calculated by using the semiclassical approximation [16–18] in which both mechanisms, Auger and resonant, are acting independently. As in previous works, we find that the interference between Auger and resonant mechanism along the ion trajectory is not important when the ground state is the only one neutralization channel [17,18]. The inclusion of excited configurations changes a little this scenario but within the experimental error bars, both calculations are similar and good enough.

In Fig. 5(a), it is shown how much the resonant neutralization to the ground state is affected by the presence of helium excited states. On the other hand, from Fig. 5(b) we can observe that the resonant neutralization to the excited states is not significant.

The very presence of the excited configurations of helium interacting with the band states affects the occupation probability of the ground state, as it can be seen from the time-dependent evolution of the Green's functions in [25]. This correlation effect can be seen more clearly in the static limit by analyzing the shift and broadening of the active levels involved, which are obtained, respectively, from the real and imaginary parts of the Fourier-transformed self-energies. In the case of the He( $1s$ ) energy level, the self-energy (only the resonant contribution) is given by [25]

$$\begin{aligned} \Sigma_{1s\sigma}(\omega) = & \Sigma_{1s}^0(\omega) + \sum_{\vec{k}} \frac{|\tilde{V}_{\vec{k}1s}|^2 (1 - n_{\vec{k}\sigma})}{\omega - \varepsilon_{\vec{k}} - i\eta} \\ & + \sum_{\vec{k}, \sigma', \alpha = s, p} \frac{|\hat{V}_{\vec{k}2\alpha}|^2 \langle n_{\vec{k}\sigma'} \rangle}{\omega - \varepsilon_{\vec{k}} + \varepsilon_{2\alpha\sigma'} - \varepsilon_{1s} - i\eta}, \end{aligned} \quad (19)$$

where the first term is the noninteracting part of the self-energy, the second is due to the spin fluctuation statistics, and the

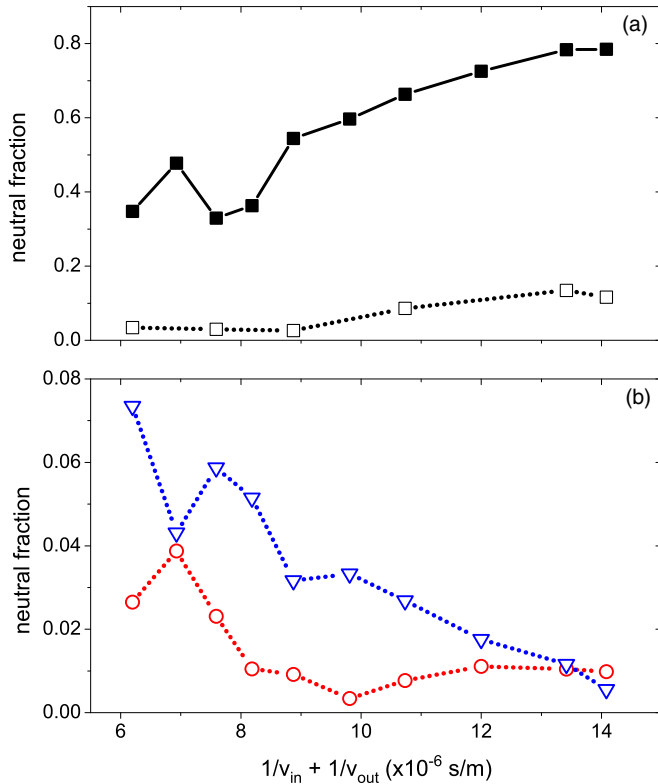


FIG. 5. (Color online) Contributions of the resonant process to the neutral fraction as a function of the inverse ion velocity. (a) Neutralization to the ground state when the excited states are considered (solid squares) and when they are disregarded (empty squares). (b) Neutralization to the excited states: He-1s2s (circles) and He-1s2p (down triangles).

third one has to be with the correlation effects introduced by the excited electronic configurations. No matter what the occupations of the excited configurations are, the width and shift of the ionization level will be affected by the presence of excited states whose energies are positioned below the Fermi level and have a non-negligible coupling with the surface states.

The expression of the self-energy associated with excited states is

$$\begin{aligned} \Sigma_{2\alpha\sigma}(\omega) = & \sum_{\bar{k}} \frac{|\hat{V}_{\bar{k}2\alpha\sigma}|^2}{\omega - \varepsilon_{\bar{k}} - i\eta} \\ & + \sum_{\bar{k}} \frac{|\hat{V}_{\bar{k}1s}|^2 \langle n_{\bar{k}\sigma} \rangle}{\omega - \varepsilon_{\bar{k}} + \varepsilon_{1s} - \varepsilon_{2\alpha\sigma} - i\eta} \\ & + \sum_{\bar{k}, (\beta\sigma') \neq (\alpha\sigma)} \frac{|\hat{V}_{\bar{k}2\beta}|^2 \langle n_{\bar{k}\sigma'} \rangle}{\omega - \varepsilon_{\bar{k}} + \varepsilon_{2\beta\sigma'} - \varepsilon_{2\alpha\sigma} - i\eta}. \end{aligned} \quad (20)$$

The corresponding atom energy levels shifted by the real part of Eqs. (19) and (20) are shown in Fig. 6 as a function of the distance to the surface. In the case of the He ground state [Fig. 6(a)], we obtain practically the same energy level when considering or not the correlation effects due to the spin statistics; the energy increase close to the surface is due to the antibonding interaction with the Al-core states (2s

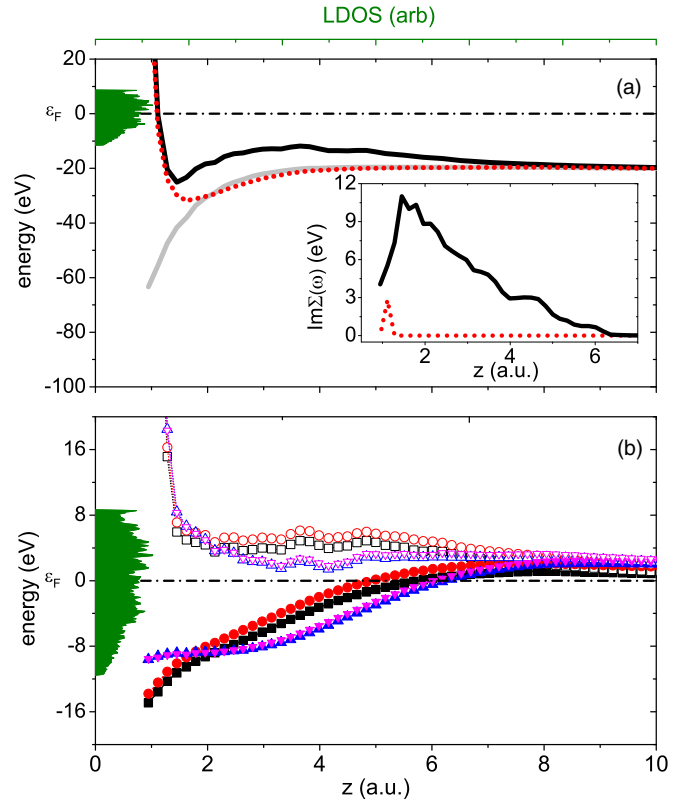


FIG. 6. (Color online) Energy levels as a function of the ion-surface distance. In panel (a): gray solid line corresponds to the adiabatic calculation of the He ionization level (see Sec. III A); dotted line to the  $\varepsilon_{1s}$  energy level shifted by the interaction with the Al-core states and by spin statistics effects [the sum of the real parts of first and second terms in Eq. (19)]; solid black line is the ion level including the shift by the correlation effects introduced by the excited states [real part of the third term in Eq. (19)]. In the inset, the widths of the shifted energy levels. In panel (b): excited energy levels:  $\varepsilon_{2s\sigma}$  (squares),  $\varepsilon_{2s\bar{\sigma}}$  (circles),  $\varepsilon_{2p,\sigma}$  (up triangles), and  $\varepsilon_{2p,\bar{\sigma}}$  (down triangles). The empty symbols correspond to the respective levels shifted by the interaction [the real part of Eq. (20)]. The shadowed region is the LDOS of Al(100).

and 2p). The interaction of the He excited states with the surface increases the energy of the He(1s) level and also its hybridization width (see inset in Fig. 6) along a large range of distances. Both results are caused by the correlation effects introduced by the excited configurations, and they lead to an increase of the probability of neutralization to the ground state, as it is observed in Fig. 5(a). In the case of the excited one-electron levels shown in Fig. 6(b), they are shifted upwards and resonate with the empty band states due to the presence of the other states interacting with the surface, justifying in this form the negligible occupation observed in Fig. 5(b).

Finally, the sensitivity to the scattering geometry when including the He excited states can be seen in Fig. 7. In this figure, we present our full calculation of the ion fraction for normal incidence in the case of a scattering angle of  $136^\circ$ , which is the scattering geometry of the experiments shown in Refs. [16,35] (both experimental results correspond to a polycrystalline surface). The results for the case of normal incidence and a scattering angle of  $180^\circ$  are also included in

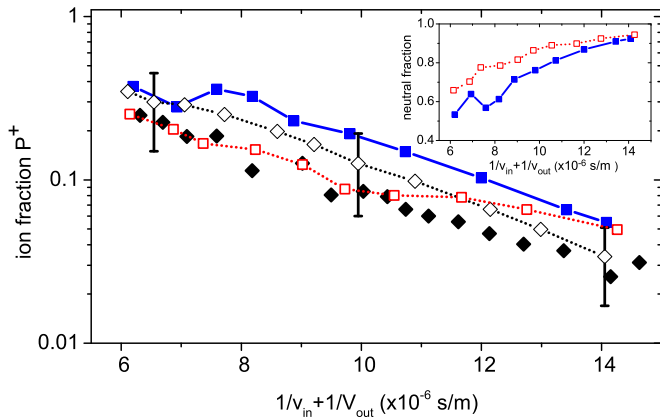


FIG. 7. (Color online) Ion fraction as a function of the inverse ion velocity. Full calculations for scattering angles of  $180^\circ/136^\circ$  (full/empty squares). Experimental data are represented by diamond symbols: Ref. [16] (empty symbols) and Ref. [35] (full symbols). In the inset, the resonant neutralization to the ground state is compared for the two scattering angles (corresponding symbols as in the main figure).

this figure for comparison. In our model calculation the ion trajectory is always normal to the surface, but the velocity corresponds to the normal component of the one in the experimental setup. Then, in the case of the scattering angle equal to  $136^\circ$ , the exit energy is diminished by the loss factor (0.6) and also by the  $\sin^2(46^\circ)$  ( $E_{\text{out}} = 0.31E_{\text{in}}$ ). A lower velocity along the outgoing trajectory means a longer time in contact with the surface and, therefore, a more probable neutralization to the ground state (see inset in Fig. 7). A smoother velocity dependence of the ion fraction is obtained in this case and the agreement with the experiment seems to be slightly improved.

## V. CONCLUSIONS

We perform a time-dependent calculation of the charge-exchange processes in  $\text{He}^+/\text{Al}$  scattering, in which we also

include the first excited states of helium and consider both mechanisms, Auger and resonant. We assume that the neutralization to the ground state is occurring via the two mechanisms, while the neutralization to the excited states is only due to resonant processes. Our starting point is an extended Anderson Hamiltonian projected over the atomic configuration space with an appreciable probability of occurrence. A Keldysh-Green functions technique is used to solve the dynamical evolution of the interacting system and obtain the ion survival probability, which is the measured quantity in the  $\text{He}^+/\text{Al}$  collision. An exhaustive analysis of the different possible calculations of the neutralization of  $\text{He}^+$  is performed: the typical one including only the ground state by either neglecting or not the electron spin, and finally the calculation which takes into account the excited configurations of helium.

We found that including the ground and excited configurations of helium within a formalism that accounts properly for the correlation effects leads to a marked upward shift of the  $\text{He}(1s)$  level and also to an increase of the hybridization width along the ion trajectory. In this form, the resonant neutralization to the ground state becomes more efficient and the agreement with the experimental results is greatly improved. We can also observe the more marked structure introduced by the resonant processes in the velocity dependence of the ion survival probability.

We also found from the comparison with the results obtained from the semiclassical approximation that the inclusion of the excited states does not introduce remarkable interference effects between the two neutralization mechanisms, resonant and Auger.

Finally, we consider that the theoretical results presented in this work together with those presented in Ref. [25] point out that the excited states of the projectile atom play an important role in the scattering of  $\text{He}^+$  by metallic surfaces.

## ACKNOWLEDGMENT

This work was supported by ANPCyT through Grant No. PICT-2010-0294, by CONICET through Grant No. PIP-201101-00621, and U.N.L. through CAI+D grants.

- 
- [1] A. Blandin, A. Nourtier, and D. Hone, *J. Phys. (Paris)* **37**, 369 (1976).
  - [2] R. Brako and D. M. Newns, *Surf. Sci.* **108**, 253 (1981).
  - [3] R. Souda, M. Aono, C. Oshima, S. Otani, and Y. Ishizawa, *Surf. Sci.* **150**, L59 (1985).
  - [4] R. Souda, M. Aono, C. Oshima, S. Otani, and Y. Ishizawa, *Surf. Sci.* **176**, 657 (1986).
  - [5] R. Souda, M. Aono, C. Oshima, S. Otani, and Y. Ishizawa, *Surf. Sci.* **179**, 199 (1987).
  - [6] R. Souda, T. Aizawa, C. Oshima, S. Otani, and Y. Ishizawa, *Phys. Rev. B* **40**, 4119 (1989).
  - [7] L. Los and J. J. C. Geerlings, *Phys. Rep.* **190**, 133 (1990).
  - [8] A. G. Borisov, D. Teillet-Billy, and J. P. Gauyacq, *Phys. Rev. Lett.* **68**, 2842 (1992).
  - [9] P. Nordlander and J. C. Tully, *Phys. Rev. B* **42**, 5564 (1990).
  - [10] D. C. Langreth and P. Nordlander, *Phys. Rev. B* **43**, 2541 (1991).
  - [11] H. Shao, D. C. Langreth, and P. Nordlander, *Phys. Rev. B* **49**, 13929 (1994).
  - [12] E. A. García, P. G. Bolcatto, and E. C. Goldberg, *Phys. Rev. B* **52**, 16924 (1995).
  - [13] L. C. A. van den Oetelaar, S. N. Mikhailov, and H. H. Brongersma, *Nucl. Instrum. Methods Phys. Res., Sect. B* **85**, 420 (1994).
  - [14] N. Lorente and R. Monreal, *Phys. Rev. B* **53**, 9622 (1996).
  - [15] J. Merino and J. B. Marston, *Phys. Rev. B* **58**, 6982 (1998).
  - [16] E. C. Goldberg, R. Monreal, F. Flores, H. H. Brongersma, and P. Bauer, *Surf. Sci.* **440**, L875 (1999).
  - [17] N. P. Wang, E. A. García, R. Monreal, F. Flores, E. C. Goldberg, H. H. Brongersma, and P. Bauer, *Phys. Rev. A* **64**, 012901 (2001).
  - [18] E. A. García, N. P. Wang, R. C. Monreal, and E. C. Goldberg, *Phys. Rev. B* **67**, 205426 (2003).

- [19] J. C. Lancaster, F. J. Kontur, G. K. Walters, and F. B. Dunning, *Phys. Rev. B* **67**, 115413 (2003).
- [20] S. Wethekam, A. Mertens, and H. Winter, *Phys. Rev. Lett.* **90**, 037602 (2003).
- [21] D. Valdes, E. C. Goldberg, J. M. Blanco, and R. C. Monreal, *Phys. Rev. B* **71**, 245417 (2005).
- [22] N. Bajales, J. Ferrón, and E. C. Goldberg, *Phys. Rev. B* **76**, 245431 (2007).
- [23] C. Meyer, F. Bonetto, R. Vidal, E. A. García, C. Gonzalez, J. Ferrón, and E. C. Goldberg, *Phys. Rev. A* **86**, 032901 (2012).
- [24] A. Iglesias-García, E. A. García, and E. C. Goldberg, *J. Phys.: Condens. Matter* **23**, 045003 (2011).
- [25] A. Iglesias-García, E. A. García, and E. C. Goldberg, *Phys. Rev. B* **87**, 075434 (2013).
- [26] H. D. Hagstrum, *Phys. Rev.* **96**, 336 (1954).
- [27] S. Tsuneyuki and M. Tsukada, *Phys. Rev. B* **34**, 5758 (1986).
- [28] R. Souda, K. Yamamoto, W. Hayami, T. Aizawa, and Y. Ishizawa, *Phys. Rev. B* **51**, 4463 (1995).
- [29] M. A. Vicente Alvarez, V. H. Ponce, and E. C. Goldberg, *Phys. Rev. B* **57**, 14919 (1998).
- [30] R. A. Baragiola, *Rad. Effects. Lett.* **61**, 47 (2006).
- [31] N. Lorente and R. Monreal, *Surf. Sci.* **370**, 324 (1997).
- [32] W. More, J. Merino, R. C. Monreal, P. Pou, and F. Flores, *Phys. Rev. B* **58**, 7385 (1998).
- [33] T. Hecht, H. Winter, and A. G. Borisov, *Surf. Sci.* **406**, L607 (1998).
- [34] R. Monreal and N. Lorente, *Phys. Rev. B* **52**, 4760 (1995).
- [35] S. Rund, D. Primetzhofer, S. N. Markin, D. Goebel, and P. Bauer, *Nucl. Instrum. Methods Phys. Res., Sect. B* **269**, 1171 (2011).
- [36] S. N. Mikhailov, R. J. M. Elfrink, J. P. Jacobs, L. C. A. van den Oetelaar, P. J. Scanlon, and H. H. Brongersma, *Nucl. Instr. Methods Phys. Res., Sect. B* **93**, 210 (1994).
- [37] A. G. Borisov, D. Teillet-Billy, and J. P. Gauyacq, *Surf. Sci.* **284**, 337 (1993).
- [38] A. G. Borisov, D. Teillet-Billy, and J. P. Gauyacq, *Surf. Sci.* **325**, 323 (1995).
- [39] G. E. Makhmetov, A. G. Borisov, D. Teillet-Billy, and J. P. Gauyacq, *Surf. Sci.* **339**, 182 (1995).
- [40] M. A. Romero, C. S. Gómez Carrillo, F. Flores, and E. C. Goldberg, *Phys. Rev. B* **87**, 195419 (2013).
- [41] E. C. Goldberg and F. Flores, *J. Phys.: Condens. Matter* **25**, 225001 (2013).
- [42] P. W. Anderson, *Phys. Rev.* **124**, 41 (1961).
- [43] P. G. Bolcatto, E. C. Goldberg, and M. C. G. Passeggi, *Phys. Rev. B* **58**, 5007 (1998).
- [44] S. Huzinaga, J. Andzelm, M. Klobukowsky, E. Radzio-Andzelm, Y. Sakai, and H. Tatewaki, in *Gaussian Basis Set for Molecular Calculation*, edited by S. Huzinaga (Elsevier, Amsterdam, 1984).
- [45] S. Huzinaga, *J. Chem. Phys.* **42**, 1293 (1965).
- [46] A. A. Radzig and B. M. Smirnov, in *Reference Data on Atoms, Molecules, and Ions*, Springer Series in Chemical Physics 31, edited by S. Huzinaga (Springer, New York, 1985).
- [47] J. P. Lewis, K. R. Glaesemann, G. A. Voth, J. Fritsch, A. A. Demkov, J. Ortega, and O. F. Sankey, *Phys. Rev. B* **64**, 195103 (2001).
- [48] P. Jelinek, H. Wang, J. P. Lewis, O. F. Sankey, and J. Ortega, *Phys. Rev. B* **71**, 235101 (2005).
- [49] L. V. Keldysh, *Zh. Eksp. Teor. Fiz.* **47**, 1515 (1964) [*Sov. Phys.—JETP* **20**, 1018 (1965)].